

## NUMERICAL COMPUTATION OF TRANSIENT SHOCKED CHEMICALLY REACTIVE FLOWS

S. RAJAN

*Department of Thermal and Environmental Engineering, Southern Illinois University, Carbondale, Illinois 62901, U.S.A.*

### SUMMARY

Using the ability of the method of characteristics to evaluate shock fronts in an accurate manner, a formulation is presented which incorporates the effect of rapid exothermic chemical reactions in the flow. The formulation is applied to the computation of the unsteady reactive flow field behind a cylindrical expanding blast wave propagating in a mixture of hydrogen and oxygen. Details of the computational procedure are described. Results are presented for a sample problem and compared with those for the non-reactive case to illustrate the influence of chemical reactions.

KEY WORDS Method of Characteristics Reactive Flows Blast Waves

### INTRODUCTION

In the computation of compressible flows governed by systems of hyperbolic equations, the method of characteristics possesses certain advantages, especially in the presence of transient shock wave interactions.<sup>1</sup> This stems from the inherent ability of the characteristics method to accurately track discontinuities in flow parameters propagated as shock waves, and discontinuities in derivatives travelling as compression or rarefaction waves. Finite difference methods, on the other hand, employ some form of artificial viscosity,<sup>2</sup> which tends to smear out the shock front over a number of grid points. Furthermore, in the proximity of travelling waves, it has been shown by Vichnevetsky<sup>3</sup> that all finite difference, finite element and method of lines schemes generate spurious numerical oscillations which can, under certain conditions, overwhelm the signal wave unless special measures are instituted to reduce their influence. Even in the steady state case, finite difference shock wave calculations with area changes have been shown to introduce significant errors.<sup>4</sup>

The ability of the method of characteristics to provide physical insight into the nature of the wave phenomena occurring in the flow has been demonstrated by a number of applications.<sup>5-7</sup> Shin and Valentin<sup>5</sup> employ approximations to the compatibility relations written in integral form along four bicharacteristics and a streamline to study the problem of a plane acoustic wave diffracting from a 90° sharp corner. A particle path formulation of the characteristic equations has been used by McLaughlin<sup>6</sup> to investigate the unsteady one-dimensional expansion of a uniform property gas into a non-uniform low density atmosphere. Flow field computations in supersonic mixed-compression aircraft inlets operating at an angle of attack have been performed by Vadyak *et al.*<sup>7</sup> using a three dimensional, discrete shock wave fitting procedure and a steady three dimensional bicharacteristic formulation of the quasilinear differential equations. Cline<sup>8</sup> has also

applied the bicharacteristics method to compute reactive nozzle flows for the hydrogen–fluorine system.

Modifications to the method of characteristics, to extend its versatility and to decrease some of the program logic complexity, include the method of near characteristics initially proposed by Sauer<sup>9</sup> and applied recently by Shin and Kot<sup>10</sup> to the hammer wave problem, and the pseudocharacteristic method of lines applied by Carver<sup>11</sup> to the shock tube problem.

Thus, although the method of characteristics in two or more independent variables has been used to compute a variety of transient and steady state flow situations, very few examples exist in the literature of its application to shocked chemically reactive flows. In this paper, the inherent advantages of the characteristics method have been used to accurately analyse the transient, chemically reactive flow behind a cylindrically expanding detonation wave. Unlike finite difference techniques, the characteristics formulation enabled the precise location of the shock to be sharply determined and the influence of rapid, simultaneous, exothermic reactions on the flow field and shock trajectory to be evaluated. Also unlike with finite difference techniques, the presence of these fast, multiple chemical reactions—the so called stiffness of the problem—does not pose any difficulties in the present method.

The problem is stated simply as follows: a strong cylindrical detonation wave initiated by a fixed strength line energy source is propagating in a reactive hydrogen–oxygen mixture diluted with argon at a specified initial temperature and pressure. Passage of the initial shock front through the gas rapidly raises the temperature and pressure and causes fast exothermic chemical reactions to occur in the shocked gas following an induction delay period. The transient *in situ* physical properties of this shocked reactive gas mixture are computed along with the shock decay trajectory at later times. A one-dimensional non-steady formulation in cylindrical co-ordinates is employed. The established kinetics of the hydrogen–oxygen system is used to arrive at the time-varying mixture composition.

The aim of the present paper is to indicate the numerical application of the method of characteristics to the analysis of transient, shocked chemically reactive flows as exemplified by the decaying detonation wave problem outlined above. Further details of the technique and the application of the method to the study of detonation wave propagation have been discussed elsewhere.<sup>12,13</sup>

## THE GOVERNING EQUATIONS

The differential equations in cylindrical co-ordinates applicable to the decaying detonation wave problem are given in<sup>13</sup> and are as follows:

$$\text{Conservation of mass:} \quad \frac{\partial \rho}{\partial t} + u \frac{\partial \rho}{\partial r} + \rho \frac{\partial u}{\partial r} + \frac{\rho u}{r} = 0 \quad (1)$$

$$\text{Conservation of momentum:} \quad \rho \frac{\partial u}{\partial t} + \rho u \frac{\partial u}{\partial r} + \frac{\partial p}{\partial r} = 0 \quad (2)$$

$$\text{Conservation of energy:} \quad \rho \frac{Dh}{Dt} - \frac{Dp}{Dt} = 0 \quad (3)$$

$$\text{Rate processes:} \quad \frac{\partial X_i}{\partial t} + u \frac{\partial X_i}{\partial r} = \frac{\omega_i}{\rho} \quad (4)$$

$$\text{Equation of state:} \quad p = \rho \sum_i X_i R_i T \quad (5)$$

The specifying equation which is found to be particularly useful in the computation of reactive

flows has been derived by Wood and Kirkwood<sup>14</sup> and is written as

$$\frac{D\rho}{Dt} = \frac{1}{a_i^2} \frac{Dp}{Dt} - \sum_{i=1}^s \left[ \left( \frac{\partial \rho}{\partial X_i} \right)_{p,T,X_j} - \frac{\rho}{C_{pr}T} \left( \frac{\partial h}{\partial X_i} \right)_{p,T,X_j} \right] \frac{DX_i}{Dt} \quad (6)$$

where the subscripts  $( )_{p,T,X_j}$  indicate that the partial derivative is evaluated with the properties kept constant at the given point. Defining  $W_c$  as

$$W_c = \sum_{i=1}^s \left[ \frac{\rho}{C_{pr}T} \left( \frac{\partial h}{\partial X_i} \right)_{p,T,X_j} - \left( \frac{\partial \rho}{\partial X_i} \right)_{p,T,X_j} \right] \frac{DX_i}{Dt}$$

the specifying equation assumes the form

$$\frac{D\rho}{Dt} = \frac{1}{a_i^2} \frac{Dp}{Dt} + W_c \quad (7)$$

### EVALUATION OF THE CHEMICAL REACTION TERM $W_c$

The term  $W_c$  incorporating the influence of chemical reaction is evaluated from the kinetics of the system. For the hydrogen–oxygen mixture used in the present example, this can be accomplished by considering a detailed kinetic scheme incorporating all possible reactions. However, this procedure often increases the complexity of the computation and invariably requires excessive computer time. To circumvent these difficulties, recourse is here made to certain simplifications to the reaction scheme peculiar to the hydrogen–oxygen system.

The reaction kinetics of the hydrogen–oxygen system has been studied extensively.<sup>15–19</sup> The reaction scheme consists of three steps, namely the initiation, chain branching and recombination

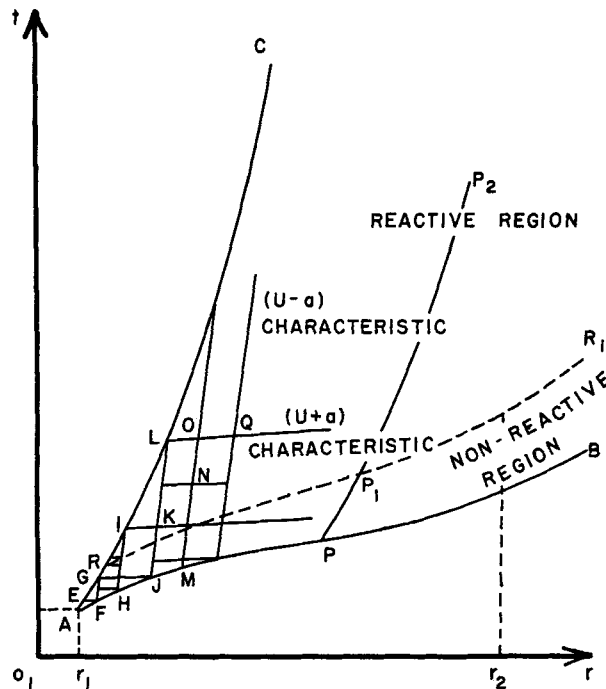


Figure 1. Computational domain and shock trajectory in  $r-t$  co-ordinates

steps. The first two steps are essentially thermally neutral. A condition of partial equilibrium has been shown to exist at the end of the chain branching step.<sup>16</sup> In the numerical calculations, therefore, the period from the passage of the shock to the end of the chain branching step—the induction period of the hydrogen–oxygen system—is considered to be non-reactive. The end of the induction period marks the beginning of the reaction front, and is shown by the line  $RR_1$  in Figure 1.

The third step of the hydrogen–oxygen reaction comprises three major recombination reactions which produce a decrease in the number of moles of the system. These recombination reactions are exothermic and represent the net heat release effects of the chemical reaction on the flow. Since there is no net mole change during the chain branching step, the extent of mole decrease during recombination is then a measure of the recombination process. This is evaluated by defining a parameter  $\nu$  as

$$\nu = \frac{N - N_{eq}}{N_i - N_{eq}} \quad (8)$$

where

$N_i$  = number of moles initially present in the unreacted system

$N$  = number of moles at a given point in the recombination region

$N_{eq}$  = number of moles at equilibrium

The value of  $\nu$  as defined above is unity at the beginning of the exothermic reactive region, and reaches an equilibrium value of zero at some distance away from the shock front.

The term  $W_c$  in the specifying equation (7) is then evaluated from local values of the recombination parameter  $\nu$ , and the initial number of moles  $N_i$  in the system. The kinetic scheme during the recombination regime needed to compute  $W_c$  is given in References 17–19.

### CHARACTERISTICS FORMULATION IN THE $(p, u, \nu)$ SYSTEM

For transient shocked chemically reactive flow, the independent variables which lend themselves most easily to the numerical computation are the pressure  $p$ , the flow velocity  $u$  and the non-dimensional reaction co-ordinate  $\nu$  defined by equation (8). Accordingly the characteristic directions and the accompanying compatibility conditions are derived with these variables in mind. The rate equation (4) and the equation of state (5) are, respectively, written in general form as

$$\frac{D\nu}{Dt} = \omega(p, \rho, \nu) \quad (9)$$

and

$$h = h(p, \rho, \nu) \quad (10)$$

Differentiating equation (10) with respect to the time  $t$  and substituting in the energy equation (3) yields

$$-\frac{1}{a_f^2} \frac{\partial p}{\partial t} - \frac{u}{a_f^2} \frac{\partial p}{\partial r} + \frac{\partial \rho}{\partial t} + u \frac{\partial \rho}{\partial r} + \frac{h_\nu}{h_\rho} \frac{\partial \nu}{\partial t} + \frac{uh_\nu}{h_\rho} \frac{\partial \nu}{\partial r} = 0 \quad (11)$$

where the frozen sound velocity

$$a_f = \frac{\rho h_p - 1}{\rho h_\rho} \quad \text{and} \quad h_p = \frac{\partial h}{\partial p} \text{ etc.} \quad (12)$$

Transformation of the continuity equation (1), the momentum equation (2) and the equation (11) to

$(\xi, \eta)$  co-ordinates gives

$$\frac{\partial \rho}{\partial \xi} \left( \frac{\partial \xi}{\partial t} + u \frac{\partial \xi}{\partial r} \right) + \frac{\partial u}{\partial \xi} \rho \frac{\partial \xi}{\partial r} = - \left( \frac{\partial \rho}{\partial \eta} \frac{\partial \eta}{\partial t} + u \frac{\partial \rho}{\partial \eta} \frac{\partial \eta}{\partial r} + \rho \frac{\partial u}{\partial \eta} \frac{\partial \eta}{\partial r} + \frac{\rho u}{r} \right) \quad (13)$$

$$\frac{\partial p}{\partial \xi} \frac{\partial \xi}{\partial r} + \frac{\partial u}{\partial \xi} \left( \frac{\partial \xi}{\partial t} + u \frac{\partial \xi}{\partial r} \right) \rho = - \left( \frac{\partial p}{\partial \eta} \frac{\partial \eta}{\partial r} + \rho \frac{\partial u}{\partial \eta} \frac{\partial \eta}{\partial t} + \rho u \frac{\partial u}{\partial \eta} \frac{\partial \eta}{\partial r} \right) \quad (14)$$

$$\begin{aligned} \frac{\partial p}{\partial \xi} \left( \frac{\partial \xi}{\partial t} + u \frac{\partial \xi}{\partial r} \right) \left( -\frac{1}{a_f^2} \right) + \frac{\partial \rho}{\partial \xi} \left( \frac{\partial \xi}{\partial t} + u \frac{\partial \xi}{\partial r} \right) \\ = \frac{1}{a_f^2} \frac{\partial p}{\partial \eta} \frac{\partial \eta}{\partial t} + \frac{u}{a_f^2} \frac{\partial p}{\partial \eta} \frac{\partial \eta}{\partial r} - \frac{\partial \rho}{\partial \eta} \frac{\partial \eta}{\partial t} - u \frac{\partial \rho}{\partial \eta} \frac{\partial \eta}{\partial r} - \frac{h_v}{h_p} \frac{\partial v}{\partial t} - \frac{h_v}{h_p} u \frac{\partial v}{\partial r} \end{aligned} \quad (15)$$

Since the characteristic lines are those along which discontinuities in  $p$ ,  $\rho$  and  $v$  propagate we can then write

$$\begin{vmatrix} \frac{\partial \xi}{\partial r} & 0 & \rho \left( \frac{\partial \xi}{\partial t} + u \frac{\partial \xi}{\partial r} \right) \\ 0 & \left( \frac{\partial \xi}{\partial t} + u \frac{\partial \xi}{\partial r} \right) & \rho \frac{\partial \xi}{\partial r} \\ \left( \frac{\partial \xi}{\partial t} + u \frac{\partial \xi}{\partial r} \right) \left( -\frac{1}{a_f^2} \right) & \left( \frac{\partial \xi}{\partial t} + u \frac{\partial \xi}{\partial r} \right) & 0 \end{vmatrix} = 0 \quad (16)$$

whence we get

$$a_f^2 \left( \frac{\partial \xi}{\partial r} \right)^2 = \left( \frac{\partial \xi}{\partial t} + u \frac{\partial \xi}{\partial r} \right)^2$$

i.e.

$$a_f \frac{\partial \xi}{\partial r} = \pm \left( \frac{\partial \xi}{\partial t} + u \frac{\partial \xi}{\partial r} \right)$$

from which we get the relation along the characteristic directions as

$$\frac{dr}{dt} = (u \pm a_f) \quad (17, 18)$$

Also (16) yields

$$\frac{\partial \xi}{\partial t} + u \frac{\partial \xi}{\partial r} = 0$$

or

$$\frac{dr}{dt} = u \quad (19)$$

as a third characteristic direction.

The characteristic directions as derived above are shown to be identical to those for non-reactive flow. Equation (3) and equations (4) and (9) are the compatibility equations along the characteristic direction  $dr/dt = u$ , i.e. along the particle path. The remaining compatibility equations along the characteristic directions  $dr/dt = (u \pm a_f)$  are derived as follows:

Rearranging equation (1) and substituting into equation (7) gives

$$\frac{\partial p}{\partial t} + u \frac{\partial p}{\partial r} + a_f^2 \rho \frac{\partial u}{\partial r} = -a_f^2 \left( W_c + \frac{\rho u}{r} \right) \quad (20)$$

Multiplying the momentum equation (2) by the frozen sound velocity  $a_f$  and rearranging we have

$$a_f \frac{\partial p}{\partial r} + a_f \rho \frac{\partial u}{\partial t} + a_f \rho u \frac{\partial u}{\partial r} = 0 \quad (21)$$

Adding equations (20) and (21) we get

$$\frac{\partial p}{\partial t} + (u + a_f) \frac{\partial p}{\partial r} + a_f \rho \left[ \frac{\partial u}{\partial t} + (u + a_f) \frac{\partial u}{\partial r} \right] = -a_f^2 \left( W_c + \frac{\rho u}{r} \right) \quad (22)$$

and subtracting (21) from (20) yields

$$\frac{\partial p}{\partial t} + (u - a_f) \frac{\partial p}{\partial r} - a_f \rho \left[ \frac{\partial u}{\partial t} + (u - a_f) \frac{\partial u}{\partial r} \right] = -a_f^2 \left( W_c + \frac{\rho u}{r} \right) \quad (23)$$

Equations (22) and (23) are the compatibility equations along the characteristic directions  $dr/dt = (u + a_f)$  and  $dr/dt = (u - a_f)$ , respectively.

Let

$$\frac{\delta^+}{\delta t} = \frac{\partial}{\partial t} + (u + a_f) \frac{\partial}{\partial r}$$

and

$$\frac{\delta^-}{\delta t} = \frac{\partial}{\partial t} + (u - a_f) \frac{\partial}{\partial r}$$

Then the compatibility equations (22) and (23) may be written as

$$\frac{\delta^+ p}{\delta t} + a_f \rho \frac{\delta^+ u}{\delta t} = -a_f^2 \left( W_c + \frac{\rho u}{r} \right) \quad (24)$$

along

$$\frac{dr}{dt} = (u + a_f)$$

and

$$\frac{\delta^- p}{\delta t} - a_f \rho \frac{\delta^- u}{\delta t} = -a_f^2 \left( W_c + \frac{\rho u}{r} \right) \quad (25)$$

along

$$\frac{dr}{dt} = (u - a_f)$$

## INITIAL AND BOUNDARY CONDITIONS

The computational domain is shown in Figure 1. AB is the shock trajectory in the  $r-t$  co-ordinate system and AC is the particle path through the initial starting point A.  $RR_1$  is the reaction front. The region  $BARR_1$  is non-reactive, corresponding to the induction zone of the hydrogen-oxygen system. Points on the reaction front  $RR_1$  are determined by computing the incremental times along a particle path  $PP_1P_2$  such that the time  $\tau_i$  elapsed during the interval  $PP_1$  is given by the

equation:

$$10^9 \log_{10} \tau_i [\text{O}_2] = \left( \frac{3565}{T} - 1.162 \right) \text{ moles l}^{-1} \text{ s}^{-1} \quad (26)$$

where  $[\text{O}_2]$  is the oxygen concentration. This is done in the calculations by evaluating the summation

$$\sum \Delta\theta = \sum \frac{\Delta t}{\tau_i} \quad (27)$$

where  $\Delta t$  is the time increment between successive points on the particle path and  $\tau_i$  is the local induction time as found from equation (26). For a point on the reaction front  $\text{RR}_1$   $\sum \Delta\theta = 1$ .

The input quantities to the computer program are

- (1) the shock Mach number at the starting point A (Figure 1)
- (2) the initial radius  $r_1$  at which the calculation is started and the final radius  $r_2$  at which it is stopped
- (3) the initial unreacted mixture composition in mole fractions
- (4) the initial ambient temperature and pressure
- (5) the thermodynamic coefficients for all the reacting species
- (6) a set of parameters used to tag the particles as they pass through the shock and continue into the reactive flow field beyond; these parameters are simply the initial radii at which they are first engulfed by the shock
- (7) a parameter  $R_0$  which controls the decay rate of the lead shock.

The parameter  $R_0$  represents the amount of energy deposited in the flow at the centre of explosion. It is computed from the blast wave theory developed by Sakurai<sup>21</sup> and is given by the equation

$$R_0 = \left( \frac{E}{P_0} \right)^{1/2} \quad (28)$$

where  $E$  is the energy per unit length supplied at the centre of the explosion and  $P_0$  is the initial pressure. The parameter  $R_0$  enters into the computation of the specified input velocity along the initial particle path AC. A smaller value of  $R_0$  causes the computed velocity along AC to decay faster. This in turn causes a faster decay in the strength of the shock front AB.

The data curves used in the method of characteristics solution are the particle path AC through the initial starting point A (Figure 1) and the shock trajectory AB. Values of  $v$  are specified along the particle path AC, in an implicit way through the compatibility equation (9). This is done by keeping track of the time that has elapsed since the particle passed through the shock. As the particle which entered the shock at A moves away from the shock front, it first traverses the induction zone AR. The point R is located by computing the total induction time from equations (26) and (27). As the particle through A proceeds into the reactive region RC, the values of  $v$  along RC are computed in an implicit way through the compatibility equation (9).

In addition to specifying  $v$  on AC, the value of the velocity  $u$  on this initial particle path is computed from the non-reactive similarity solution of Sakurai,<sup>21</sup> for an expanding cylindrical blast wave using the Mach number at point A. By specifying the velocity  $u$  and the recombination parameter  $\nu$  on the initial particle path, we have in effect prescribed a piston velocity sustaining the shock motion, together with the law of chemical reaction along this particle path.

Since the curve CAB is crossed by both the left running and right running characteristics with compatibility equations (22) and (23), and we have already specified two of the dependent

variables—namely  $u$  and  $v$ —on AC, it is possible to specify the value of  $p$  alone on the data curve AB. This is done indirectly by solving the relevant compatibility equation (22) and the Rankine–Hugoniot equations obtaining across the shock trajectory AB.

### CALCULATION PROCEDURE

Figure 2 is a schematic representation of the calculation procedure. The computations are initiated at point A, Figure 1, at a specified initial shock Mach number. The properties of the shocked gas at A are obtained by solving the non-reactive Rankine–Hugoniot equations. Using the velocity of the

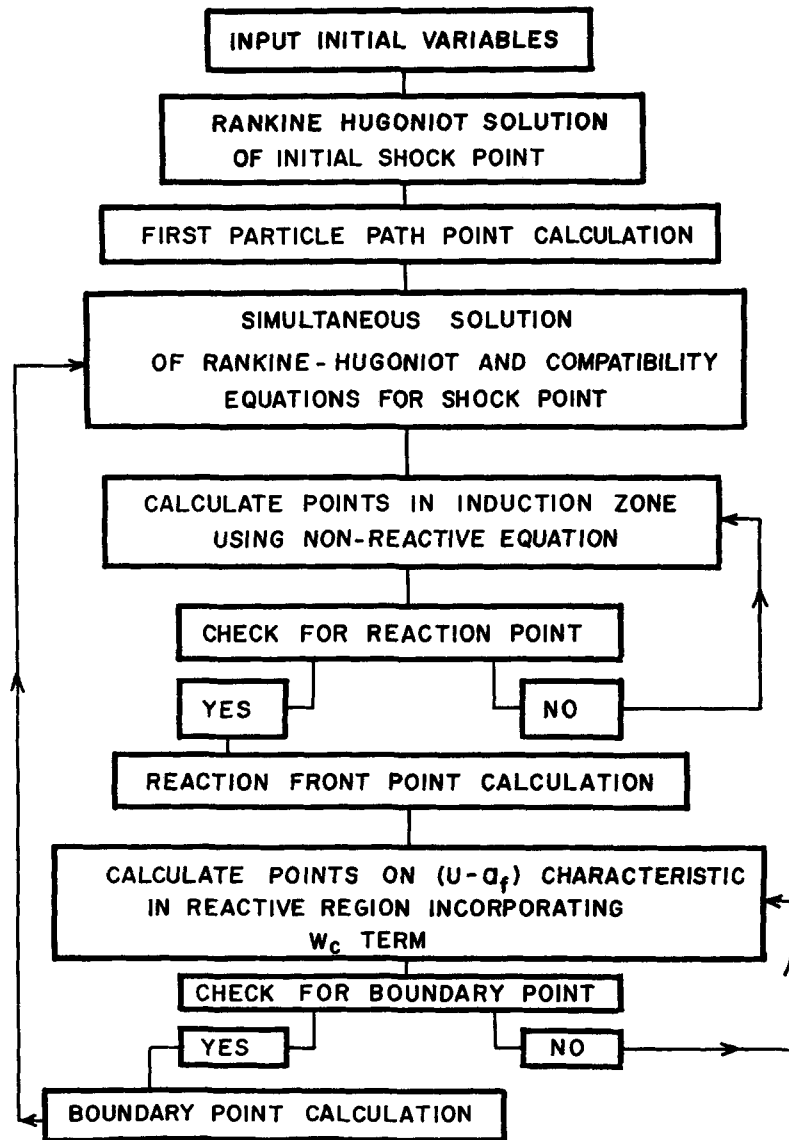


Figure 2. Schematic diagram of the computational procedure

shocked gas at A, point E on the initial particle path AC after a time interval  $\Delta t$  is obtained. From E the point F on the shock trajectory is computed by solving simultaneously the compatibility condition (24) along the  $(u + a_f)$  characteristic EF and the Rankine–Hugoniot conditions for the non-reactive shock point F. Points are then computed along the  $(u - a_f)$  characteristic FG until the point G on the limiting particle path AC is reached. Next, points on the  $(u - a_f)$  characteristic HI are computed from known points along FG until points in the entire flow field BAC have been calculated.

Calculation of a boundary point such as G is accomplished by employing the known properties at points E and F and the relevant compatibility equations. The compatibility equations to be satisfied are equations (3) and (9) along EG and equation (24) along FG. Since G lies in the non-reactive induction zone, equation (9) assumes the form.

$$\frac{Dv}{Dt} = 0$$

The term  $W_c$  in equation (24) is also not evaluated at point G. However, it is included in the computation of a boundary point in the reactive region such as I or L.

In the computation of boundary points such as G, I and L, it is necessary to furnish the particle velocity at these points. This is done by assuming that the decaying detonation wave is a strong blast wave and employing the series solution of Sakurai<sup>21</sup> to compute the particle velocity of these points.

In the process of calculation of points along a  $(u - a_f)$  characteristic, the situation usually arises that as the reaction front is approached, a mesh point such as 12'3'5 shown in Figure 3 is encountered. The calculation of point 2 on the reaction front poses certain problems because it lies on the boundary separating the reactive and non-reactive regions of the flow. To locate the point 2 exactly on the reaction front, a calculation is first made on the assumption that points 2' and 3' lie in the reactive region and point 2' is located by using the proper compatibility relations along 1-2' and 3'-2'. Next the particle path is drawn backwards through 2' to intersect the  $(u - a_f)$  characteristic 5-1 at 4'. The fractional induction time at 2' is then evaluated by adding the fractional induction time from 4'-2' to that at point 4'. A check is now made to see if the fractional induction time at 2' is equal to unity. If the fractional induction time is more than one, which is usually the case, point 3' is now brought closer to point 5 and the whole procedure repeated

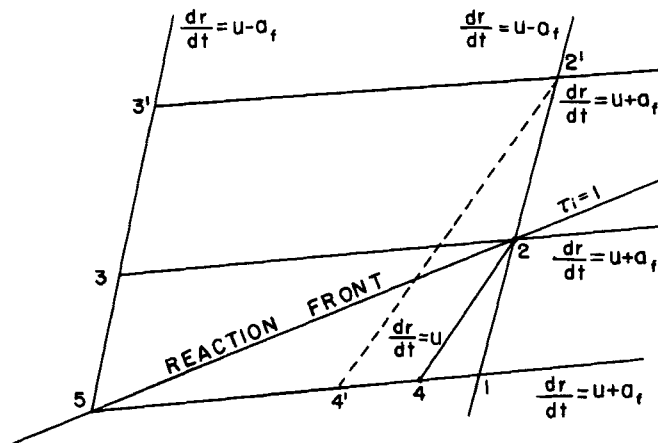


Figure 3. Characteristics net for a point on the reaction front

iteratively until the fractional induction time at 2 on the reaction front satisfies the condition

$$|\tau_{i2} - 1.00| \leq 0.005$$

The compatibility equations employed in the solution are

$$\begin{aligned} \frac{\delta^+ p}{\delta t} + a_f \rho \frac{\delta^+ u}{\delta t} &= -a_f^2 \left( W_c + \frac{\rho u}{r} \right) && \text{along 3-2} \\ \frac{\delta^- p}{\delta t} - a_f \rho \frac{\delta^- u}{\delta t} &= -a_f^2 \frac{\rho u}{r} && \text{along 1-2} \\ \rho \frac{Dh}{Dt} - \frac{Dp}{Dt} &= 0 && \text{along 4-2} \end{aligned} \tag{29}$$

Point 2 in Figure 4 depicts a typical net point such as Q in the reactive region CRR<sub>1</sub> (Figure 1). For such a mesh point calculation in the reactive region, equations (30) to (32) represent the finite difference forms of the compatibility equations (24), (25) and (9), respectively. The compatibility equations employed in the solution written in finite difference form are

$$\frac{p_2 - p_3}{t_2 - t_3} + (a_f \rho)_{32} \frac{u_2 - u_3}{t_2 - t_3} = -a_{f,32}^2 \left( W_c + \frac{\rho u}{r} \right)_{32} \tag{30}$$

along the  $(u + a_f)$  characteristic 3-2,

$$\frac{p_2 - p_1}{t_2 - t_1} - (a_f \rho)_{12} \frac{u_2 - u_1}{t_2 - t_1} = -a_{f,12}^2 \left( W_c + \frac{\rho u}{r} \right)_{12} \tag{31}$$

along the  $(u - a_f)$  characteristic 1-2, and

$$\frac{dv}{dt} = f(\rho, T, v) \quad \text{or} \quad \frac{v_2 - v_4}{t_2 - t_4} = f(\rho, T, v) \tag{32}$$

along the particle path 4-2.

The term  $W_c$  appearing in equation (30) is taken as the average of the values for points 2 and 3 in Figure 4, whereas for equation (31) it is taken as the average of the values for points 1 and 2.

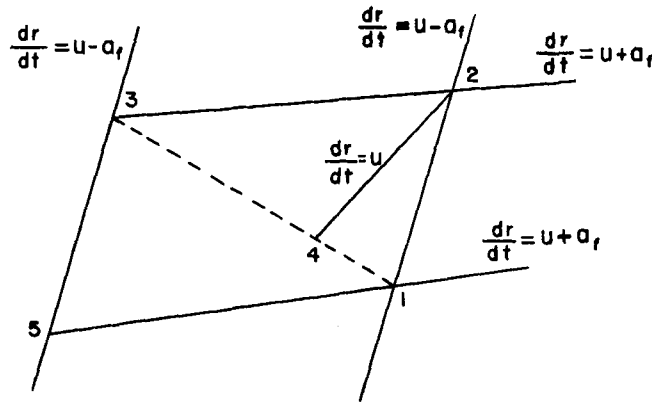
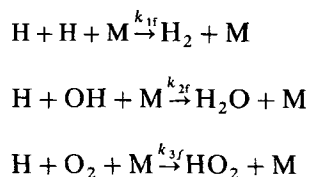


Figure 4. Characteristics net for a point in the reactive region

Table I. Chemical reactions occurring during recombination



M = Third body not entering into reaction.

The form of equation (32) is given by Getzinger and Schott<sup>17</sup> for reactions of the type



The reaction scheme employed for the recombination regime is that used in Reference 13 and consists of three reactions which are listed in Table I. The reverse rates  $k_{jr}$  are computed from the forward rates  $k_{jf}$  and the appropriate equilibrium constants.

Points 1 and 3 have been completely determined from previous computations. Point 2 is located from known values at points 1 and 3 by purely geometric considerations. The evaluation of the requisite quantities at point 2 involves four sets of iterations and is performed in elemental steps in eight subroutines, some of which are common to other steps in the overall calculations. Two iterations are required to satisfy the three compatibility equations above, and the calculation of the temperature  $T$  and the species composition at 2 require one iteration each making four iterations in all.

Values for  $u_2$ ,  $a_2$ ,  $v_2$ ,  $p_2$  and  $T_2$  are first assumed as the average of the corresponding values at points 1 and 3; of these the values of  $u_2$ ,  $p_2$  and  $v_2$  are taken to be reference values to be compared with calculated values at the end of the iteration. Using the assumed values of  $v_2$ ,  $T_2$  and  $p_2$  the species composition in mole fractions of the reacting mixture is calculated, and the term  $W_c$  evaluated.

At this point all the terms involved in the compatibility equations, (30) and (31) are known except  $p_2$  and  $u_2$ . We therefore solve equations (30) and (31) to find new values of  $p_2$  and  $u_2$ . The point 4 on the particle path through 2 is now located and values of  $p_4$ ,  $T_4$ ,  $v_4$  and  $\tau_{i4}$  are found. The third compatibility equation (32) along the particle path is solved to find a new value for  $v_2$ , after which the temperature  $T_2$  is calculated by iteration on the basis of the energy equation (3). A check is now made to see if the new values of  $p_2$ ,  $u_2$  and  $v_2$  agree simultaneously within specified limits with the chosen reference values so labelled at the outset of the calculation. If this condition is not satisfied, the newly obtained values of  $p_2$ ,  $u_2$  and  $v_2$  are now labelled as reference values and the iteration is repeated, until the values of  $p_2$ ,  $u_2$  and  $v_2$  at the end of an iteration agree within the specified limits with the corresponding values at the beginning of the iteration. The increment in induction time for the segment 4-2 is now found and added on to  $\tau_{i4}$  to find the induction time  $\tau_{i2}$  at point 2.

Calculation of points on a  $(u - a_t)$  characteristic lying within the induction zone defined by B-A-R-R<sub>1</sub> is performed in a similar manner to the computation of the reaction point described above, except that the term  $W_c$  in equations (30) and (31) is set equal to zero and the compatibility equation (32) is not used.

Control of the mesh size was maintained to attain good accuracy in the presence of rapidly varying property variables in the reactive region. If the variation in any one of the quantities  $p_2$ ,  $u_2$

or  $v_2$  at point 2 in Figure 4 was more than five per cent of the values at point 1, a new point was added midway between points 5 and 3, the whole numbering sequence along the  $(u - a_f)$  characteristic 5-3 was changed and the point 2 recalculated. If, however, the variation in the calculated values  $p_2$ ,  $u_2$  and  $v_2$  was less than one per cent of the values at 1, the point was recalculated using the next higher point above 3 on the previous  $(u - a_f)$  characteristic. As the total time for a single problem took anywhere from thirty to ninety minutes on the IBM 360/70 machine, it was expedient to maintain the net size at its optimum value. The number of mesh points on each  $(u - a_f)$  characteristic was governed by the above criterion that the variation in the properties  $p$ ,  $u$  and  $v$  not exceed five per cent from those at the previous mesh point. The number of mesh points also depended on the distance between the shock trajectory AB and the particle path AC, and varied anywhere from 5 to 50 points.

The method of solution of the characteristic equations described above differs from the constant time increment procedure of Hartree<sup>22</sup> employed by Chou *et al.*<sup>23</sup> and the modified Hartree technique used by McLaughlin.<sup>7</sup> However, in the presence of chemical reactions the straightforward iterative procedure as employed in this paper was found expedient to maintain adequate control of the mesh size to ensure good accuracy in regions where the properties were subject to rapid variations.

### NUMERICAL RESULTS

The transient decaying detonation wave problem addressed here constitutes a rigorous test of the numerical technique as it couples the rapid composition and temperature changes from chemical reaction with the unsteady cooling effects of flow expansion in the presence of a shock. In the numerical results presented, the shock Mach number at the initial starting point A (Figure 1) is 9. This Mach number yielded shocked gas temperatures which were within the range of the JANNAF thermodynamic tables<sup>24</sup> used in the computations to evaluate the enthalpies, etc. The initial gas mixture consisted of stoichiometric hydrogen and oxygen diluted with fifty per cent by volume of

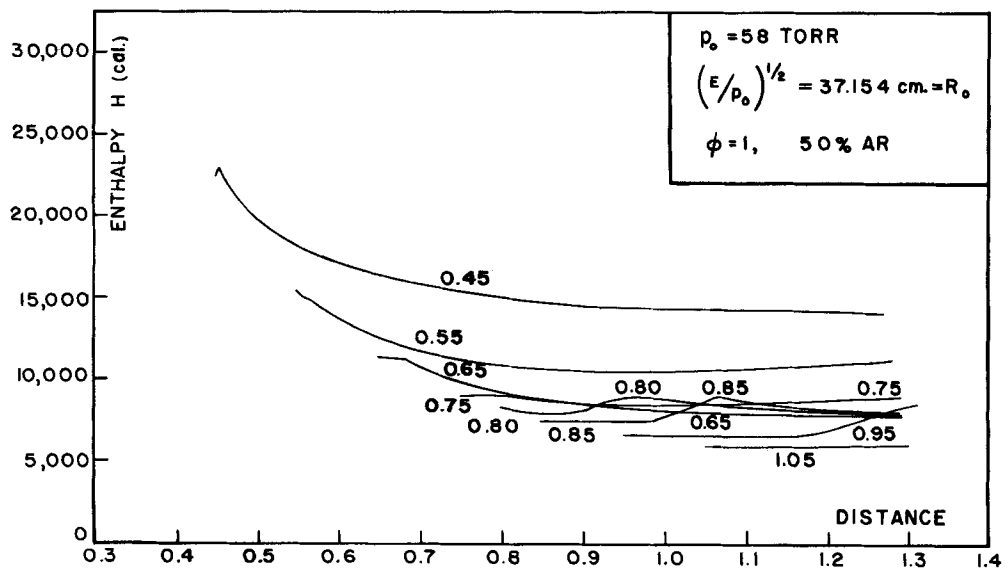


Figure 5. Variation of enthalpy along particle paths, reactive case

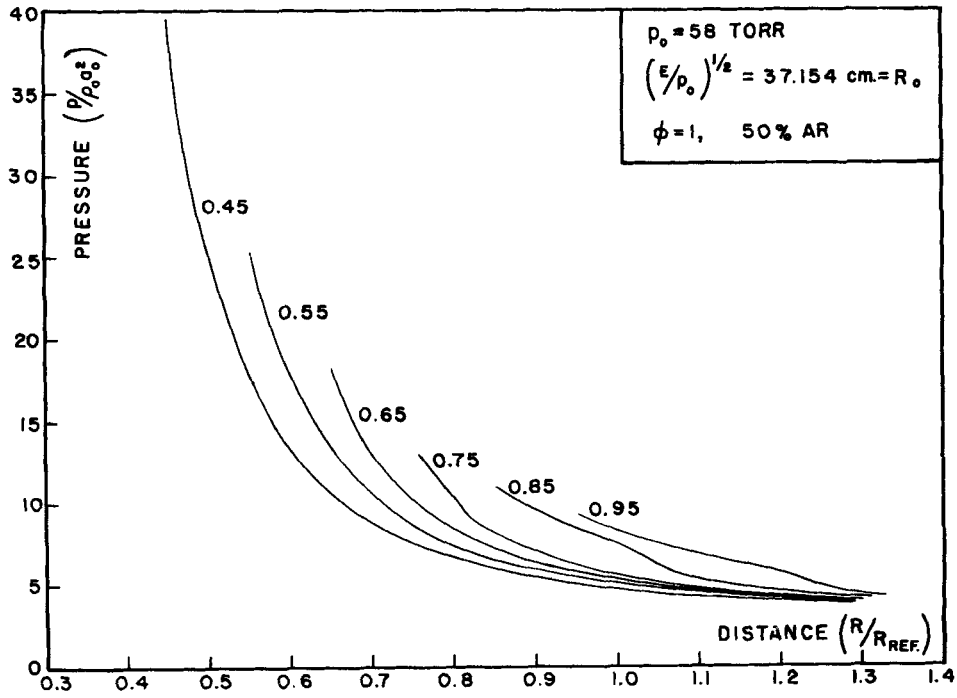


Figure 6. Variation of pressure along particle paths, reactive case

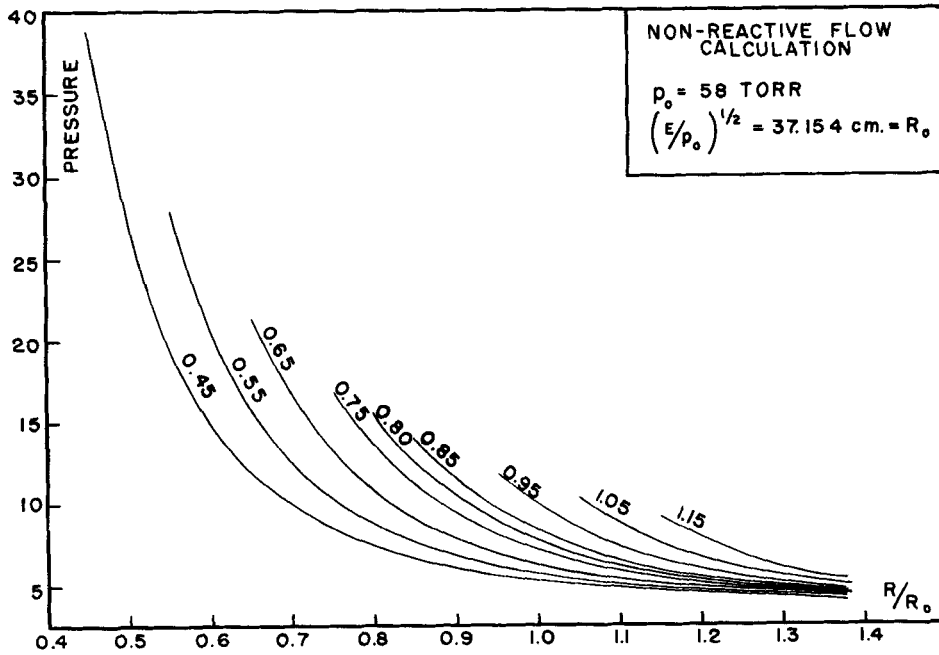


Figure 7. Variation of pressure along particle paths, non-reactive case

argon. The initial temperature and pressure used in the calculations were 300° K and 58 mm of mercury, respectively. The value of the decay parameter  $R_0$  representing the blast energy  $E$  (equation (28)) was 37.154 cm.

The rapid flow expansion caused by the high initial shock Mach number usually caused the temperature and other gas-dynamic parameters to drop quickly behind the shock in the region around A (Figure 1). This necessitated that the net size be kept as small as possible in this region to get reliable results. Further on where the shock front was weaker and its decay rate less marked, a larger net size could be employed. This control of net size was accomplished by a checking procedure in the calculation of a shock point in the computer program.

Figure 5 shows the variation of enthalpy along different particle paths as a function of the non-dimensional radius defined as  $R/R_0$ . The numbers labelled on each curve represent the non-dimensional radius at which the particle was first engulfed by the shock. The particle path labelled 0.45 in Figure 5 is close to the centre of explosion where the flow expansion effects are predominant. Hence the heat release effects of chemical reaction are not apparent on this curve. Further away from the centre of the explosion, where the cooling flow expansion effects are not so strong, the enthalpy rise due to exothermic chemical reaction can be seen, as for example on the curves labelled 0.8, 0.85 etc. The initial essentially horizontal portions of these curves represent the region during which the particle is undergoing an induction period, which is considered non-reactive in the present calculations. Comparison of the curves labelled 0.80, 0.85, 0.95, etc. reveal that this induction period becomes longer as the strength of the shock front decays with distance.

Since the method of characteristics furnishes a unique solution,<sup>25</sup> and the literature does not contain solutions corresponding to the reactive flow problems presented here, a comparison was made between the reactive and non-reactive flows to further illustrate the influence of exothermic chemical reactions. Figures 6 and 7 show the non-dimensional pressure along different particle paths for the reactive and non-reactive cases, respectively. All input conditions to the computer program were the same in the two cases as shown in the Figures, except that the computation of the term  $W_c$  was suppressed in the non-reactive case.

Figure 7 shows that the non-dimensional pressure along particle paths attenuates smoothly in

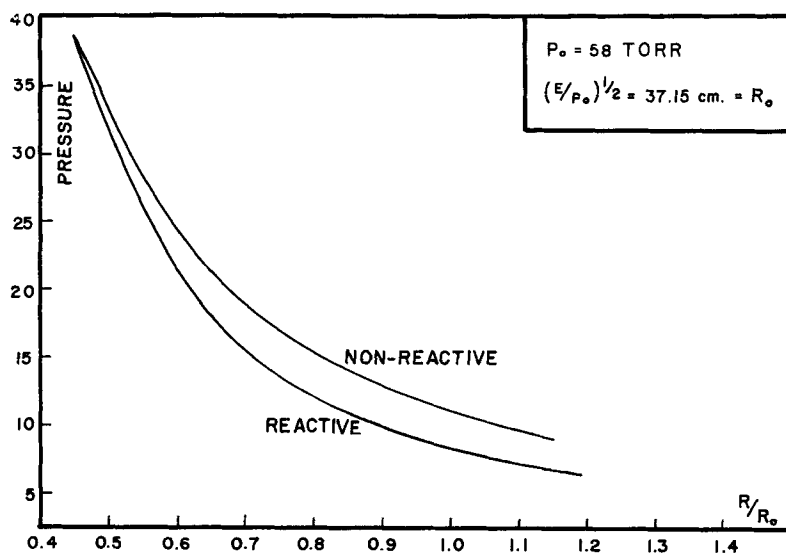


Figure 8. Comparison of pressure immediately behind the shock front with and without chemical reaction

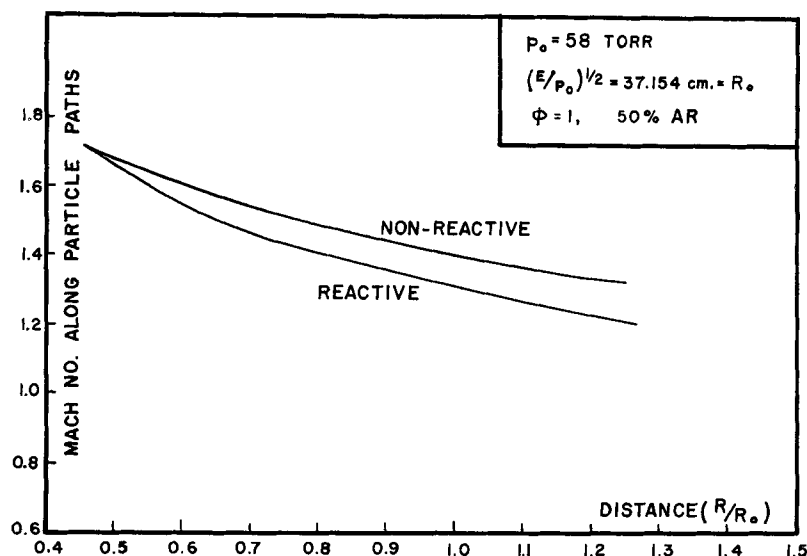


Figure 9. Comparison of flow Mach number immediately behind the shock front with and without chemical reaction

the non-reactive case, as is to be expected. The pressure variation along particle paths in the reactive case, Figure 6, distinctly illustrates the effect of chemical reaction. As in the case of the enthalpy curves shown in Figure 5, these effects are more predominant at distances further away from the centre of explosion as exemplified by the particle paths that entered the shock at non-dimensional radii of 0.75 and 0.85. A distinct change of slope occurs in the pressure curve at the end of the induction period. The pressure drops more rapidly during the initial induction period, but the curves flatten out showing that, in the reactive region, the pressure along particle paths decays less rapidly.

Figures 8 and 9 show the variation of pressure and flow Mach number respectively immediately behind the shock front for the reactive and non-reactive cases. The Figures illustrate the influence of chemical reaction in the flow on the shock decay rate at later times. Figure 9 reveals that the shock front decays faster with chemical reaction occurring in the flow. This faster shock front decay produces lower pressures in the shocked gas immediately adjacent to the shock front as depicted in Figure 8.

## CONCLUSIONS

A characteristics formulation in  $(p, u, v)$  variables has been presented and applied to the unsteady propagation of a decaying detonation wave in a reactive hydrogen-oxygen mixture. The characteristics method employed here enables the shock trajectory to be accurately determined. Comparison of the computed results for the reactive and non-reactive cases illustrates the influence of chemical reactions on the flow field and on the shock trajectory at later times. It is found that the shock front decays faster in the presence of exothermic reactions as compared to the non-reactive case.

The numerical computation of flow fields involving the coupling of the chemical rate processes with the unsteady gas dynamics, such as the decaying detonation wave problem illustrated here, poses a challenge in that it involves two classes of physical phenomena whose time scales can be widely different. In other studies, this problem of widely varying time scales of the chemical and

fluid mechanical phenomena has been addressed by employing a time-step splitting technique, as used for instance by Oran *et al.*<sup>26</sup> in their solution of the shock tube problem with chemical reaction. They use the flux-corrected transport algorithm developed by Boris<sup>27</sup> to solve the fluid dynamic equations. This enables the shock front to be resolved in one or two cells with minimal numerical diffusion. In comparison, the method of characteristics solution described herein avoids the time splitting procedure and enables the shock front to be sharply and accurately defined. The characteristics formulation is particularly suited to the computation of unsteady chemically reactive flows in the presence of shocks, as it simplifies the program logic in the solution of problems involving widely varying chemical reaction and fluid mechanical time scales.

#### ACKNOWLEDGEMENTS

The author would like to acknowledge helpful discussions with Professor Roger A. Strehlow during the numerical computation.

#### NOTATION

$a_f$	Frozen composition sound velocity
A, B, D	Chemical species in recombination reaction
C	Third body in chemical reaction
$C_{pf}$	Frozen composition specific heat at constant pressure
$h$	Enthalpy per unit mass
$k_{jf}$	Forward recombination rate for reaction $j$
$M$	Mach number
$N$	Number of moles
$P$	Pressure
$r$	Space co-ordinate
$R$	Gas constant
$R_0$	Blast wave decay parameter
$S$	Total number of recombination reactions
$t$	Time co-ordinate
$T$	Temperature
$u$	Flow velocity
$W_c$	Quantity describing the effect of chemical reaction
$X_j$	Mole fraction of species $j$
$\Delta$	Incremental value
$\Delta\theta$	Fraction of delay time used in calculations
$\phi$	Stoichiometry on fuel/air basis
$\tau_i$	Fractional induction time
$\rho$	Density, gm/cm <sup>3</sup>
$v$	Dimensionless parameter indicating the extent of recombination of the H <sub>2</sub> -O <sub>2</sub> system
$\omega_i$	Rate of change of species $i$ defined by equation (4)
[ ]	Concentration, moles/l
$\frac{\partial( )}{\partial[ ]}$	Partial derivative of ( ) w.r.t. [ ]
$\frac{D( )}{D[ ]}$	Total Derivative of ( ) w.r.t. [ ]

- $\frac{\delta^+}{\delta t}$  ( ) Directional derivative of ( ) in the direction  $dr/dt = (u + a)$
- $\frac{\delta^-}{\delta t}$  ( ) Directional derivative of ( ) in the direction  $dr/dt = (u - a)$

## REFERENCES

1. N. E. Hoskin and B. D. Lambourn, 'The computation of general problems in one dimensional unsteady flow by the method of characteristics', in J. Ehlers *et al.* (eds.), *Lecture Notes in Physics, Proceedings of the Second International Conference on Numerical Methods in Fluid Dynamics*, Springer-Verlag, 1970.
2. J. von Neumann and R. D. Richtmyer, 'A method for the numerical calculation of hydrodynamic shocks', *J. Applied Physics*, **21**, 232–237 (1950).
3. R. Vichnevetsky and B. Peiffer, in R. Vichnevetsky, (ed.), *Advances in Computer Methods for Partial Differential Equations*, AAICA Press, Rutgers University, New Brunswick, N.J., 1975, p. 52.
4. I. G. Cameron, 'An analysis of the errors caused by using artificial viscosity terms to represent steady state shock waves', *J. Computational Physics*, **7**, 1–20 (1966).
5. Y. W. Shin and R. A. Valentin, 'Numerical analysis of fluid-hammer waves by the method of characteristics', *J. Computational Physics*, **20**, 220–237 (1976).
6. R. McLaughlin, 'The numerical solution of the unsteady expansion of a gas into a near vacuum', *J. Computational Physics*, **35**, 77–89 (1980).
7. J. Vadyak, J. D. Hoffman and A. R. Bishop, 'Flow computations in inlets at incidence using a shock fitting bicharacteristic method', *AIAA Journal*, **18**, 1495–1502 (1980).
8. M. J. Cline, 'The analysis of non-equilibrium chemically reacting supersonic flow in 3-dimensions using a bicharacteristics method', *J. Computational Physics*, **12**, 1 (1973).
9. R. Sauer, 'Differenzenverfahren für hyperbolische Anfangswert probleme bei mehr als zwei unabhängigen Veränderlichen mit Hilfe von Nebencharakteristiken', *Numerische Mathematik*, **5**, 55–67 (1963).
10. Y. W. Shin and C. A. Kot, 'Two-dimensional fluid-transient analysis of the method of nearcharacteristics', *J. Computational Physics*, **28**, 211–231 (1978).
11. M. B. Carver, 'Pseudo characteristic method of lines solution of the conservation equations', *Journal of Computational physics*, **35**, 57–70 (1980).
12. S. Rajan, 'On the interaction between chemical kinetics and gas dynamics in the flow behind a cylindrical detonation front', *Ph.D. Thesis*, University of Illinois, Urbana, 1970.
13. S. Rajan and R. A. Strehlow, 'Effect of chemical reactions in the shocked gas on the propagation characteristics of cylindrical detonation waves', *Combustion and Flame*, **49**, (1), 73–90 (1983).
14. W. W. Wood and J. Kirkwood, 'Hydrodynamics of a reacting and relaxing fluid', *Applied Physics*, **28**, 395–398 (1957).
15. G. L. Schott, 'Kinetic studies of hydroxyl radicals in shock waves. II. Induction times in the hydrogen–oxygen reaction', *J. Chem. Physics*, **29**, 117–1182 (1958).
16. G. L. Schott, 'Kinetic studies of hydroxyl radicals in shock waves III. The OH concentration maximum in the hydrogen–oxygen reaction', *J. Chem. Physics*, **32**, 710–716 (1960).
17. R. W. Getzinger and G. L. Schott, 'Recombination via the  $H + O_2 + M \rightarrow HO_2 + M$  Reaction in lean hydrogen–oxygen mixtures', *J. Chem. Physics*, **43**, 3237–3246 (1965).
18. G. L. Schott and P. F. Bird, 'Kinetic studies of hydroxyl radicals in shock waves. IV. Recombination rates in rich hydrogen–oxygen mixtures', *J. Chem. Physics*, **41**, 2869–2875 (1964).
19. R. W. Getzinger, 'A shock wave study of recombination in near-stoichiometric hydrogen–oxygen mixtures', *Eleventh Symposium (International) on Combustion*, The Combustion Institute, 1967, pp. 117–124.
20. R. A. Strehlow and A. Cohen, 'Initiation of detonation', *Physics of Fluids*, **5**, 97–101 (1962).
21. A. Sakurai, 'Blast wave theory' in M. Holt (ed.) *Basic Developments in Fluid Dynamics*, Volume 1, Academic Press, (1965).
22. D. R. Hartree, *Numerical Analysis*, 2nd edn, Oxford University Press, London/New York, 1958.
23. P. C. Chou, R. R. Karpp and S. L. Huang, 'Numerical calculation of blast waves by the method of characteristics', *AIAA Journal*, **5**, 618–623 (1967).
24. D. R. Stull and H. Prophet, *JANNAF Thermochemical Tables*, 2nd edn, National Bureau of Standards, 1971.
25. R. Courant, *Partial Differential Equations*, Vol. 2 of *Methods of Mathematical Physics*, Interscience Publishers, 1962.
26. E. Oran, T. Young and J. Boris, 'Application of time-dependent numerical methods to the description of reactive shocks', *Seventeenth Symposium (International) on Combustion*, The Combustion Institute, 1978, pp. 43–54.
27. J. P. Boris and D. L. Book, *Methods in Computational Physics*, Vol. 16, Academic Press, 1976, pp. 85–129.